Optimization of the Attenuation Coefficient for Chang Attenuation Correction in ^{123}I Brain Perfusion SPECT

Taisuke Murata[1,2], Yuri Hayashi[1], Masahisa Onoguchi[2], Takayuki Shibutani[2], Takashi Iimori[1], Koichi Sawada[1], Tetsuro Umezawa[1], Yoshitada Masuda[1], and Takashi Uno[3]

[1]Department of Radiology, Chiba University Hospital, Chiba, Japan; [2]Department of Quantum Medical Technology, Graduate School of Medical Sciences, Kanazawa University, Kanazawa, Japan; and [3]Department of Diagnostic Radiology and Radiation Oncology, Graduate School of Medicine, Chiba University, Chiba, Japan

N-isopropyl-*p*-^{123}I-iodoamphetamine brain perfusion SPECT has been used with various attenuation coefficients (μ-values); however, optimization is required. This study aimed to determine the optimal μ-value (μ_{opt}-value) for Chang attenuation correction (AC) using clinical data by comparing the Chang method and CT-based AC. **Methods:** We used 100 patients (reference group, 60; disease group, 40) who underwent *N*-isopropyl-*p*-^{123}I-iodoamphetamine SPECT. SPECT images of the reference group were obtained to calculate the AC using the Chang method (μ-values, 0.07–0.20; 0.005 interval) and the CT-based method, both without scatter correction (SC) and with SC. The μ_{opt}-value with the smallest mean percentage error for the brain regions of the reference group was calculated. Agreement between the Chang and CT-based methods applying the μ_{opt}-value was evaluated using Bland–Altman analysis. Additionally, the percentage error in the region of hypoperfusion in the diseased group was compared with the percentage error in the same region in the reference group when the μ_{opt}-value was applied. **Results:** The μ_{opt}-values were 0.140 for Chang without SC and 0.160 for Chang with SC. In the Chang method, with the μ_{opt}-value applied, fixed and proportional biases were observed in the Bland–Altman analysis (both $P < 0.05$), and there was a tendency for the percentage error to be underestimated in the limbic regions and overestimated in the central brain regions. There was no significant difference between the disease group and the reference group in the region of hypoperfusion in either Chang without SC or Chang with SC. **Conclusion:** The present study revealed that the μ_{opt}-values of the Chang method are 0.140 without SC and 0.160 with SC.

Key Words: SPECT; brain perfusion; Chang attenuation correction

J Nucl Med Technol 2023; 51:49–56
DOI: 10.2967/jnmt.122.264990

Brain perfusion SPECT is required to be qualitatively and quantitatively accurate. SPECT projection data are subject to scattering and attenuation of γ-rays caused by the subject. Particularly, attenuation causes a depth-dependent decrease in counts within the subject, leading to significant accuracy errors in quantitative evaluation (*1*). Therefore, attenuation correction (AC) is vital to obtain accurate brain perfusion SPECT images.

CT-based AC (a nonuniform AC) and Chang AC (a uniform AC) are used mainly in brain perfusion SPECT. The CT-based method is considered the gold standard for AC because of its high correction accuracy. Contrastingly, the Chang method is widely used in routine clinical practice primarily because of its simplicity in AC processing. It does not require a CT scan, thereby eliminating radiation exposure. The attenuation map of the Chang method is given by a constant attenuation coefficient (μ-value) for each radionuclide energy. Various μ-values have been used for *N*-isopropyl-*p*-^{123}I-iodoamphetamine brain perfusion SPECT, with variations (broad-beam: 0.07 (*2*), 0.08 (*3*), 0.09 (*4*), and 0.10 (*5*); narrow-beam: 0.11 (*3*), 0.12 (*6*), 0.146 (*2,5,7*), 0.160 (*8*), 0.166 (*9*), and 0.167 (*10*)). Optimization of μ-values is required for the Chang method in *N*-isopropyl-*p*-^{123}I-iodoamphetamine brain perfusion SPECT.

It is necessary to consider the effect of skull attenuation (*11–13*) and the difference in μ-value depending on the slice position (*9,12,14*) to optimize the μ-value of the Chang method. The skull is relatively thicker in the occipital region than in other regions (*15*), making it difficult to reproduce the actual skull thickness in the phantom accurately. Additionally, when μ-values are determined using a pooled phantom, the basal ganglia level is the evaluation target (*16*), resulting in inadequate evaluation of the parietal and cerebellar levels. Van Laere et al. (*13,17*) noted that μ-values determined experimentally using phantoms cannot be directly extrapolated for application to clinical data.

This study aimed to determine the optimal μ-value (μ_{opt}-value) using clinical data. The μ-value that most closely approximates the AC effect of the CT-based method, the gold standard, was determined as the μ_{opt}-value of the Chang method. We further validated the μ_{opt}-value by evaluating agreement between the Chang and CT-based methods when μ_{opt}-values were applied and by evaluating the error of the μ_{opt}-values in hypoperfusion regions.

MATERIALS AND METHODS

This retrospective study was approved by our institution's ethics review committee. All data used for analysis were obtained from

Received Oct. 4, 2022; revision accepted Jan. 17, 2023.
For correspondence or reprints, contact Masahisa Onoguchi (onoguchi@staff.kanazawa-u.ac.jp).

routine clinical diagnostic investigations; no other examinations were performed for the study. The requirement for written consent was waived by the ethics review committee.

Patients

This study included 100 patients (male, 47; female, 53; median age, 66.0 y [range, 23.1–90.3 y]) who underwent *N*-isopropyl-*p*-^{123}I-iodoamphetamine brain perfusion SPECT between January and December 2021. Patients diagnosed with generally preserved perfusion or mild nonspecific hypoperfusion were defined as the reference group. Patients diagnosed with specific hypoperfusion were defined as the disease group. The reference group included 60 patients (male, 28; female, 32; median age, 63.5 y [23.1–90.3 y]), and the disease group included 40 patients (male, 19; female, 21; median age, 72.5 y [48.4–88.2 y]). Disease groups included Alzheimer disease, dementia with Lewy bodies, frontotemporal lobar degeneration, and multiple-system atrophy of the cerebellar type, with 10 patients each. Patients with diseases other than the above and equivocal hypoperfusion were excluded from being selected for the disease groups.

Data Acquisition and Reconstruction

All patients were administered 111 MBq of *N*-isopropyl-*p*-^{123}I-iodoamphetamine, and the SPECT scan was obtained using a dual-head γ-camera (NM/CT 870 DR hybrid SPECT/CT scanner; GE Healthcare) equipped with an extended low-energy general-purpose collimator. The energy peak was set at 159 keV with a 20% energy window. The subwindow for scatter correction (SC) was set at 20% centered at 130 keV. SPECT scans were obtained with the following parameters: continuous-acquisition mode, 360° circular orbit, 90 projections of a 4° step angle, an 180-s acquisition per cycle for 8 cycles, a radius rotation of 150 mm, and 64 × 64 matrices with a zoom magnification of ×2.0. CT scans for AC were obtained with the following acquisition and reconstruction parameters: helical scan mode, tube voltage of 120 kVp, tube current of 40 mA, 0.5 s of rotation time, and slice thickness of 3.75 mm (matrix, 512 × 512; pixel size, 0.97 mm). The CT data were converted with bilinear scaling to attenuation maps corresponding to 159 keV using the scanner software.

All patient SPECT projection data were reconstructed using ordered-subset expectation maximization (OSEM; 5 iterations and 10 subsets). The reconstructions for each patient included OSEM plus the Chang method (ChangAC), OSEM plus the Chang method plus SC (ChangACSC), OSEM plus the CT-based method (CTAC), and OSEM plus the CT-based method + SC (CTACSC). For ChangAC and ChangACSC, AC was performed by varying the μ-values from 0.07 to 0.20 (0.05 intervals). A threshold process for each patient determined the contour of the attenuation map when performing the Chang method. The threshold value whose contour was nearest the outer edge of the skull was adopted by referring to the CT images (*12*). The dual-energy window method was used for SC (*18*). The pixel size of the reconstructed SPECT image was 4.42 mm, and the slice thickness was also 4.42 mm. A Butterworth filter (cutoff, 0.5 cycles/cm; order, 8) was used for smoothing.

Data Analysis

All SPECT images were analyzed using AZE Virtual Place HAYABUSA software (Canon Medical Systems), and 3-dimensional stereotactic surface projection analysis was performed. To avoid anatomic standardization errors, the head tilt was adjusted to the anterior commissure–posterior commissure line (*19,20*). Counts of 37 brain regions were measured using volume-of-interest templates incorporated into the 3-dimensional stereotactic surface projection on anatomically standardized SPECT images. The 37 brain regions included were the left and right parietal lobes, temporal lobe, frontal lobe, occipital lobe, posterior cingulate gyrus, anterior cingulate gyrus, medial frontal lobe, medial parietal lobe, medial temporal lobe, sensorimotor cortex, visual cortex, caudate nucleus, cerebellum, cerebellar vermis, putamen, parahippocampal gyrus, amygdala, thalamus, and pons (not divided into left and right).

Determination of μ_{opt}-Value

The percentage error of each brain region for ChangAC/CTAC pairs and ChangACSC/CTACSC pairs was calculated for the reference group:

$$\text{Percentage error} = \frac{\text{count}_{\text{ChangAC,ChangACSC}} - \text{count}_{\text{CTAC,CTACSC}}}{\text{count}_{\text{CTAC,CTACSC}}}.$$

First, the mean percentage error for all brain regions (37 volumes of interest) was calculated for each patient. The μ-value with the smallest mean percentage error was the μ_{opt}-value for each patient. The number distribution of the μ_{opt}-values for each patient was determined to identify the range of individual differences.

Next, the mean percentage error of all brain regions (2,220 volumes of interest) in the 60 reference patients was calculated. The absolute value of the percentage error in each brain region was also calculated to identify the magnitude of the error. Additionally, unsuitable μ-values with significant differences from those of the CT-based method were identified by comparing the counts of all brain regions in ChangAC/CTAC pairs and ChangACSC/CTACSC pairs.

Bland–Altman analysis was performed on each pair of counts to evaluate agreement between ChangAC (with μ_{opt}-value)/CTAC pairs and between ChangACSC (with μ_{opt}-value)/CTACSC pairs. The percentage error of each pair was also identified for each brain region.

Validation of μ_{opt}-Values

SPECT images of the disease group with ChangAC and ChangACSC with μ_{opt}-values were used. The percentage error in the hypoperfusion region for the ChangAC/CTAC and ChangACSC/CTACSC pairs was calculated and compared with the percentage error in the same region in the reference group. The hypoperfusion regions were defined as the posterior cingulate gyrus and medial temporal lobe for Alzheimer disease, the occipital lobe for dementia with Lewy bodies, the frontal and temporal lobes for frontotemporal lobar degeneration, and the cerebellum for multiple-system atrophy of the cerebellar type.

Statistical Analysis

Statistical analyses were performed using JMP Pro (version 16.1.0; SAS Institute). The difference in counts between ChangAC/CTAC pairs and ChangACSC/CTACSC pairs with varying μ-values for the Chang method was evaluated using the Wilcoxon signed-rank test. Fixed and proportional biases for ChangAC/CTAC pairs and ChangACSC/CTACSC pairs were evaluated using Bland–Altman analysis. A paired *t* test and linear regression analysis were used to analyze the fixed and proportional biases, respectively, on the Bland–Altman plots. The percentage error of the disease and reference groups for ChangAC/CTAC pairs and ChangACSC/CTACSC pairs in the hypoperfusion region was evaluated using the Wilcoxon signed-rank test. For all statistical analyses, a *P* value of less than 0.05 was considered statistically significant.

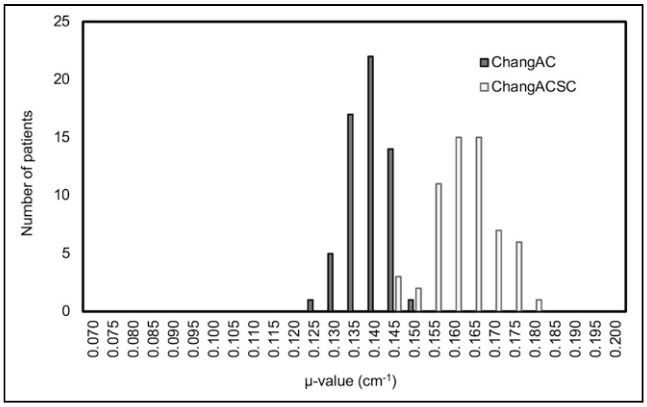

FIGURE 1. Distribution of number of μ_{opt}-values per patient in reference group.

RESULTS

The distribution of the number of μ_{opt}-values per patient in the reference group is shown in Figure 1. The μ_{opt}-values differed among patients. In ChangAC, the μ_{opt}-values ranged from 0.125 to 0.150, with 0.140 being the most common value. In ChangACSC, the μ_{opt}-values ranged from 0.145 to 0.180, with 0.160 and 0.165 being the most common values.

The percentage error of ChangAC in the reference group is listed in Table 1, and Table 2 shows the percentage error of ChangACSC. ChangAC exhibited the smallest percentage error with CTAC with a μ-value of 0.140, whereas ChangACSC displayed the smallest percentage error with CTACSC with a μ-value of 0.160. For both ChangAC and ChangACSC, smaller μ-values tended to underestimate counts, and larger μ-values resulted in overestimated counts. The maximum absolute percentage error was 22.81% for ChangAC with a μ-value of 0.140 and 31.63% for ChangACSC with a μ-value of 0.160. Comparison of counts between the Chang and CT-based methods revealed significant differences in all μ-values except 0.140 for ChangAC and 0.160 and 0.165 for ChangACSC.

Agreement between ChangAC applying a μ_{opt}-value of 0.140 and CTAC and between ChangACSC applying a μ_{opt}-value of 0.160 and CTACSC in the reference group are shown in Figures 2A and 2B. We identified a positive fixed bias between ChangAC and CTAC and a negative fixed bias between ChangACSC and CTACSC (both $P < 0.05$). Therefore, there was an overall overestimation trend for ChangAC and an underestimation trend for ChangACSC. Linear regression analysis revealed a proportional bias for ChangAC and ChangACSC (both $P < 0.05$).

TABLE 1
Percentage Error and Absolute Percentage Error Between ChangAC Applying Each μ-Value and CTAC

μ-value	Percentage error	Absolute percentage error	*P*
0.070	−38.22 ± 4.02 (−46.17, −29.28)	38.22 ± 4.02 (29.28, 46.17)	<0.05
0.075	−36.13 ± 3.90 (−46.51, −28.14)	36.13 ± 3.90 (28.14, 46.51)	<0.05
0.080	−33.78 ± 3.85 (−42.76, −25.84)	33.78 ± 3.85 (25.84, 42.76)	<0.05
0.085	−31.40 ± 3.64 (−41.03, −22.94)	31.40 ± 3.64 (22.94, 41.03)	<0.05
0.090	−28.75 ± 3.66 (−39.59, −19.08)	28.75 ± 3.66 (19.08, 39.59)	<0.05
0.095	−26.24 ± 3.34 (−36.81, −19.01)	26.24 ± 3.34 (19.01, 36.81)	<0.05
0.100	−23.78 ± 3.10 (−35.49, −16.19)	23.78 ± 3.10 (16.19, 35.49)	<0.05
0.105	−21.01 ± 3.03 (−32.43, −12.95)	21.01 ± 3.03 (12.95, 32.43)	<0.05
0.110	−18.24 ± 2.79 (−32.14, −9.23)	18.24 ± 2.79 (9.23, 32.14)	<0.05
0.115	−15.40 ± 2.50 (−25.94, −6.05)	15.40 ± 2.50 (6.05, 25.94)	<0.05
0.120	−12.12 ± 3.59 (−25.31, 1.84)	12.12 ± 3.59 (0.16, 25.31)	<0.05
0.125	−9.00 ± 3.94 (−22.25, 7.01)	9.07 ± 3.78 (0.06, 22.25)	<0.05
0.130	−5.85 ± 4.40 (−19.93, 14.24)	6.38 ± 3.58 (0.00, 19.93)	<0.05
0.135	−2.45 ± 4.95 (−17.42, 18.89)	4.54 ± 3.13 (0.00, 18.89)	<0.05
0.140	0.96 ± 5.62 (−13.92, 22.81)*	4.45 ± 3.57 (0.00, 22.81)*	0.58
0.145	4.18 ± 6.78 (−10.06, 28.65)	6.14 ± 5.07 (0.00, 28.65)	<0.05
0.150	8.13 ± 6.93 (−8.82, 35.49)	8.58 ± 6.37 (0.00, 35.49)	<0.05
0.155	11.95 ± 7.74 (−6.43, 38.81)	12.06 ± 7.57 (0.00, 38.81)	<0.05
0.160	15.86 ± 8.57 (−3.87, 49.12)	15.87 ± 8.54 (0.13, 49.12)	<0.05
0.165	19.92 ± 8.88 (−1.74, 52.43)	19.92 ± 8.87 (0.01, 52.43)	<0.05
0.170	23.93 ± 9.61 (1.83, 56.66)	23.93 ± 9.61 (1.83, 56.66)	<0.05
0.175	28.23 ± 10.50 (4.85, 64.57)	28.23 ± 10.50 (4.85, 64.57)	<0.05
0.180	32.72 ± 11.41 (8.26, 70.96)	32.72 ± 11.41 (8.26, 70.96)	<0.05
0.185	37.16 ± 12.69 (6.29, 82.40)	37.16 ± 12.69 (6.29, 82.40)	<0.05
0.190	42.19 ± 13.82 (13.63, 91.62)	42.19 ± 13.82 (13.63, 91.62)	<0.05
0.195	46.63 ± 14.82 (13.69, 99.40)	46.63 ± 14.82 (13.69, 99.40)	<0.05
0.200	52.23 ± 16.26 (20.34, 107.87)	52.23 ± 16.26 (20.34, 107.87)	<0.05

*Smallest mean percentage error and absolute percentage error.
Data are mean ± SD, followed by range in parentheses.

TABLE 2
Percentage Error and Absolute Percentage Error Between ChangACSC Applying Each μ-Value and CTACSC

μ-value	Percentage error	Absolute percentage error	*P*
0.070	−45.25 ± 5.28 (−60.55, −23.14)	45.25 ± 5.28 (23.14, 60.55)	<0.05
0.075	−43.35 ± 5.31 (−61.10, −21.36)	43.35 ± 5.31 (21.36, 61.10)	<0.05
0.080	−41.39 ± 5.34 (−56.87, −18.13)	41.39 ± 5.34 (18.13, 56.87)	<0.05
0.085	−39.25 ± 5.31 (−53.72, −15.78)	39.25 ± 5.31 (15.78, 53.72)	<0.05
0.090	−37.34 ± 5.35 (−55.51, −14.08)	37.34 ± 5.35 (14.08, 55.51)	<0.05
0.095	−35.15 ± 5.34 (−49.77, −11.23)	35.15 ± 5.34 (11.23, 49.77)	<0.05
0.100	−32.88 ± 5.33 (−50.07, −9.59)	32.88 ± 5.33 (9.59, 50.07)	<0.05
0.105	−32.92 ± 7.79 (−56.93, −6.89)	32.92 ± 7.79 (6.89, 56.93)	<0.05
0.110	−28.30 ± 5.44 (−48.50, −5.35)	28.30 ± 5.44 (5.35, 48.50)	<0.05
0.115	−26.04 ± 5.60 (−45.59, −2.26)	26.04 ± 5.60 (2.26, 45.59)	<0.05
0.120	−23.26 ± 5.71 (−43.11, −0.11)	23.26 ± 5.71 (0.11, 43.11)	<0.05
0.125	−20.84 ± 6.01 (−41.59, 3.75)	20.86 ± 5.96 (0.02, 41.59)	<0.05
0.130	−18.40 ± 5.69 (−39.99, 4.84)	18.42 ± 5.61 (0.03, 39.99)	<0.05
0.135	−15.66 ± 5.92 (−36.30, 8.17)	15.74 ± 5.70 (0.02, 36.30)	<0.05
0.140	−13.43 ± 5.85 (−35.95, 10.34)	13.56 ± 5.54 (0.01, 35.95)	<0.05
0.145	−10.56 ± 6.29 (−29.52, 13.57)	10.99 ± 5.51 (0.05, 29.52)	<0.05
0.150	−7.58 ± 6.67 (−29.75, 19.25)	8.65 ± 5.21 (0.01, 29.75)	<0.05
0.155	−4.40 ± 7.33 (−26.91, 26.51)	7.04 ± 4.85 (0.01, 26.91)	<0.05
0.160	−1.11 ± 7.94 (−27.83, 31.63)*	6.37 ± 4.88 (0.01, 31.63)*	0.06
0.165	2.26 ± 8.76 (−20.46, 39.34)	6.97 ± 5.76 (0.01, 39.34)	0.05
0.170	5.63 ± 9.40 (−19.51, 42.13)	8.37 ± 7.07 (0.02, 42.13)	<0.05
0.175	9.39 ± 10.45 (−16.02, 50.41)	10.88 ± 8.88 (0.04, 50.41)	<0.05
0.180	12.99 ± 11.28 (−19.97, 62.12)	13.76 ± 10.32 (0.00, 62.12)	<0.05
0.185	17.09 ± 11.83 (−11.97, 64.69)	17.33 ± 11.46 (0.02, 64.69)	<0.05
0.190	20.98 ± 12.77 (−10.09, 69.26)	21.10 ± 12.57 (0.00, 69.26)	<0.05
0.195	24.45 ± 13.11 (−16.22, 72.17)	24.51 ± 12.98 (0.08, 72.17)	<0.05
0.200	28.34 ± 14.13 (−11.36, 86.37)	28.37 ± 14.07 (0.05, 86.37)	<0.05

*Smallest mean percentage error and absolute percentage error.
Data are mean ± SD, followed by range in parentheses.

The percentage error in each brain region for ChangAC applying a μ_{opt}-value of 0.140 and CTAC and for ChangACSC applying a μ_{opt}-value of 0.160 and CTACSC in the reference group is shown in Figure 3. In both ChangAC and ChangACSC, some brain regions in the limbic region were underestimated (the right temporal lobe, right frontal lobe, and right sensorimotor cortex and, bilaterally, the parietal lobes, occipital lobes, and visual cortex), and some brain regions in the central region tended to be overestimated (pons and, bilaterally, the medial temporal lobes, caudate nucleus, pons, putamen, parahippocampal gyrus, and thalamus).

Examples of SPECT images of reference patients with ChangAC/CTAC and ChangACSC/CTACSC are shown in Figures 4A and 4B. ChangAC and ChangACSC tended to slightly overestimate the central brain regions and underestimate the limbic cortex in the μ_{opt}-value in series normalization. In CT-based method normalization, the μ_{opt}-value produced SPECT images more similar to the CT-based method than did the conventionally used μ-values.

Table 3 summarizes the percentage error results in the hypoperfusion region for ChangAC applying a μ_{opt}-value of 0.140 and ChangACSC applying a μ_{opt}-value of 0.160. The percentage error in the hypoperfusion region for each disease group did not significantly differ from that of the same region in the reference group for either ChangAC or ChangACSC.

DISCUSSION

We determined μ_{opt}-values in ChangAC and ChangACSC retrospectively using clinical data. The μ_{opt}-values were 0.140 for ChangAC and 0.160 for ChangACSC. However, some brain regions were under- or overestimated in the SPECT images when the μ_{opt}-values were applied. Limitations of the Chang method, as a uniform AC, were also revealed.

The distribution of μ_{opt}-values per patient displayed some variation, with 0.140 being the most common value for ChangAC and 0.160 and 0.165 being most common for ChangACSC. However, it is not practical to apply individual μ-values for each patient. Therefore, we determined μ_{opt}-values by averaging out the variation in patients by analyzing all brain regions together in 60 reference patients. By comparing the counts of the Chang method with those of the CT-based method, we identified significant differences for all μ-values except 0.140 in ChangAC and 0.160 and 0.165 in ChangACSC, thereby providing statistical support for the μ_{opt}-value. Stodilka et al. (*12*) reported a relative

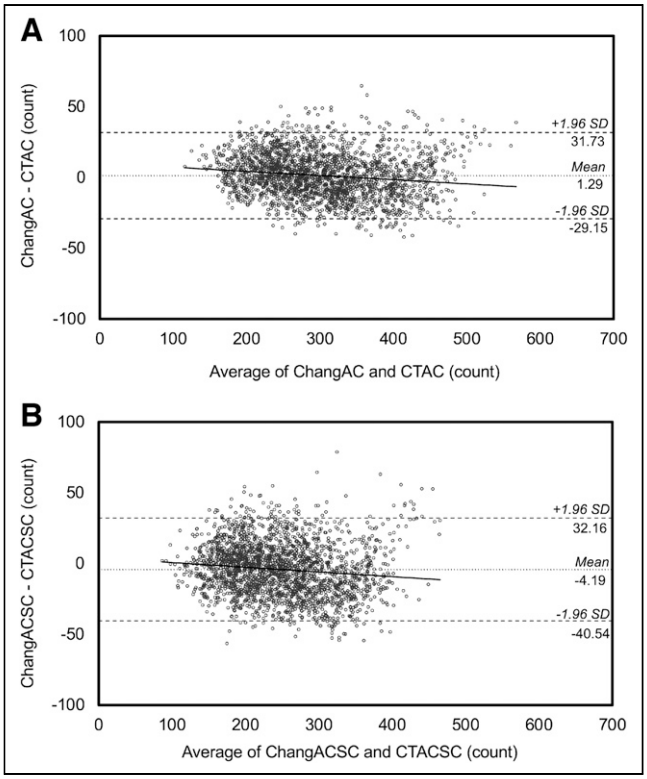

FIGURE 2. Results of Bland–Altman analysis comparing ChangAC applying μ_{opt}-value of 0.140 and CTAC (A) and comparing ChangACSC applying μ_{opt}-value of 0.160 and CTACSC in reference group (B). Solid lines show regressions; 95% limits of agreement are represented by dashed lines. 95% CIs were 0.66 to 1.92 (A) and −4.95 to −3.44 (B).

quantification error of 20% by applying a μ-value of 0.120 to ChangAC in a phantom study. In the present patient-based study, the absolute percentage error for ChangAC applying the μ_{opt}-value was 22.81%. Although the degree of error was comparable, the μ_{opt}-values for phantoms and patients were different. For quantitation using ^{123}I, Iida et al. reported a maximum percentage error of 30% for ChangAC with a μ-value of 0.090 and for ChangACSC with a μ-value of 0.166 (*9*). For ChangAC, a smaller percentage error was achieved by applying the μ_{opt}-value in this study. For ChangACSC, there was no noticeable difference from this study because the μ-values were close to our μ_{opt}-values. Interindividual variability of anatomic standardization in brain perfusion SPECT is 3%–9% (*21–23*). The absolute percentage error between the CT-based and Chang methods in the present study averaged 4.45% for ChangAC and 6.37% for ChangACSC. Application of the μ_{opt}-values achieved an AC error comparable to the interindividual variation of anatomic standardization that can occur in routine clinical practice.

Bland–Altman analysis revealed systematic bias in ChangAC and ChangACSC when applying the μ_{opt}-value, and agreement with the CT-based method was not perfect. The percentage error for ChangAC and ChangACSC tended to be underestimated in the limbic brain regions and overestimated in the central brain regions. This trend was visually confirmed in an example of the SPECT image of a reference patient shown in Figure 4. Ito et al. (*4*) reported an overestimation of central brain regions in ChangACSC applying a μ-value of 0.166, relatively close to our μ_{opt}-value. These facts highlight the limitations of the Chang method even when using μ_{opt}-values and reiterate the superiority of the CT-based method.

The skull possesses a higher μ-value than brain tissue because of greater photon loss. Further, the thickness of the skull varies slightly with age and sex (*24*). The different μ_{opt}-values per patient in the present study appear to be due to skull thickness variations among patients. Nicholson et al. (*11*) reported that the skull paradoxically affects broad-beam μ-values, and other studies (*12,13*) also reported lower μ-values than those of uniform soft tissue. Stodilka et al. (*12*) observed that μ_{opt}-values at the cerebellar level, surrounded by thick bony structures, are smaller than those at the basal ganglia level. Iida et al. (*9*) reported smaller μ-values at the cerebellar level, where the airway is included in the slice position, and higher μ-values at the parietal level, where the skull is relatively thick. These reports indicate a complex

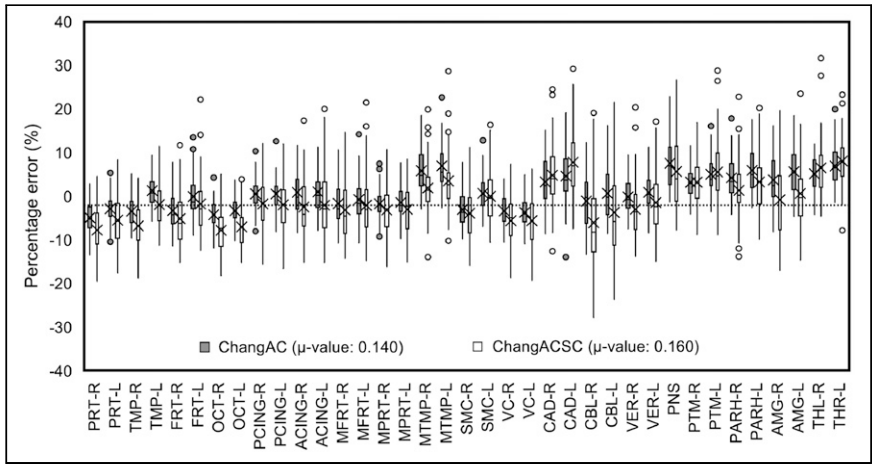

FIGURE 3. Percentage error in each brain region for ChangAC applying μ_{opt}-value of 0.140 and CTAC and for ChangACSC applying μ_{opt}-value of 0.160 and CTACSC in reference group. Dotted line indicates zero. For ChangAC and ChangACSC, limbic brain regions tended to be underestimated and central brain regions overestimated. PRT = parietal lobe; TMP = temporal lobe; FRT = frontal lobe; OCT = occipital lobe; PCING = posterior cingulate gyrus; ACING = anterior cingulate gyrus; MFRT = medial frontal lobe; MPRT = medial parietal lobe; MTMP = medial temporal lobe; SMC = sensorimotor cortex; VC = visual cortex; CAD = caudate nucleus; CBL = cerebellum; VER = cerebellar vermis; PNS = pons; PTM = putamen; PARH = parahippocampal gyrus; AMG = amygdala; THL = thalamus.

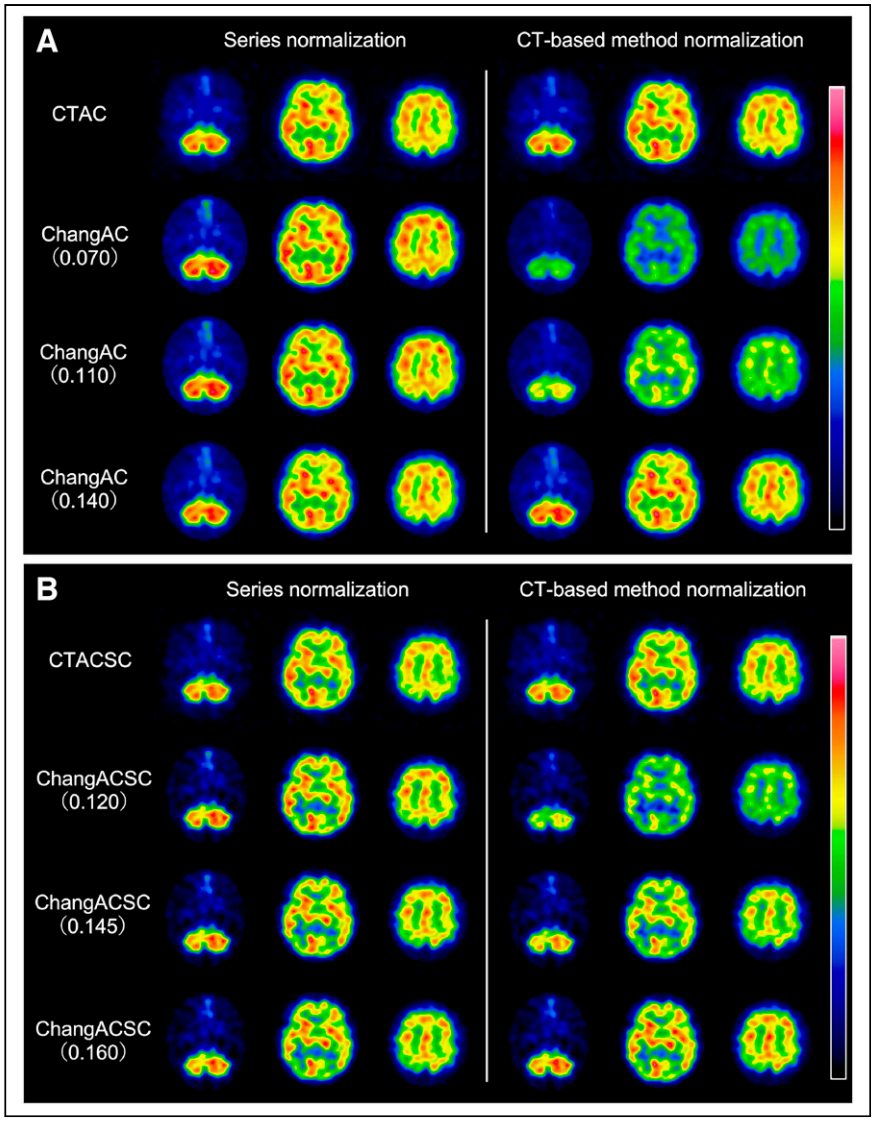

FIGURE 4. Comparison of SPECT images of CTAC and ChangAC (A) and CTACSC and ChangACSC (B) in 1 reference patient. For ChangAC, μ-values of 0.07, 0.110, and 0.140 were applied; for ChangACSC, μ-values of 0.12, 0.145, and 0.160 were applied. On left are SPECT images normalized by maximum counts in series; on right are SPECT images normalized by maximum counts of CT-based method. From left to right, axial slices are at cerebellar, basal ganglia, and parietal levels.

interplay of several factors involved in optimizing μ-values. In this study, we averaged the differing μ_{opt}-values in patients by a combined analysis of 60 reference patients and accounted for differences in correction error among brain regions by analyzing all brain regions together using anatomic standardization. Our method provides a generalizable μ_{opt}-value that considers differences in skull thickness (an error factor for interpatient variation) and differences in attenuation structure for each imaging slice position (an error factor for intrapatient variation). Consequently, the μ_{opt}-value determined in the present study is relatively high compared with the various μ-values conventionally used.

The theoretic narrow-beam μ-value for water for the 159-keV γ rays emitted by ^{123}I is 0.148 (*25*). Using the theoretic narrow-beam μ-value for ChangAC overcorrects for attenuation and overestimates the brain center region (*26*). Harris et al. (*27*) reported that a slightly lower μ-value should be applied than the theoretic μ-value. Here, the μ_{opt}-value of ChangAC was also lower than the theoretic narrow-beam μ-value.

The μ_{opt}-value of ChangACSC in our study was higher than the theoretic narrow-beam μ-value, whereas previous studies proposed lower values than the theoretic narrow-beam μ-value (*12,13,16*). Some previous studies using phantoms focused on assessing the uniformity of AC (*12,16*) because brain perfusion SPECT images are commonly normalized by the maximum count in the series. The uniformity of AC contributes to qualitative improvement. In this study using clinical data, the SD of the percentage error at low μ-values was small, and uniformity within the series was preserved. Contrarily, the absolute percentage error applying μ_{opt}-values was comparable to that reported by Stodilka et al. (*12*), indicating that quantification was assured. Iida et al. (*9*) reported no apparent difference in regional CBF images obtained with the measured attenuation map and ChangACSC applying a high μ-value of 0.166. Therefore, it is difficult for the Chang method to achieve both qualitative and quantitative performance because low μ-values contribute to qualitative improvement whereas high μ-values contribute to quantitative improvement. Since the degree of contribution of high μ-values to the quantitation improvement was greater than the degree of contribution of low μ-values to the qualitative improvement, using high μ-values is recommended.

We validated the μ_{opt}-value determined using the reference group in hypoperfusion regions to confirm their adaptability to the disease group. The choice of target diseases was considered so that the entire brain region (anterior, posterior, lateral, parietal, and basal regions) could be included as hypoperfusion regions. We observed no significant difference in the percentage error in the hypoperfusion regions in the reference and disease groups when the μ_{opt}-value was applied, indicating adaptability of the μ_{opt}-value for the disease group.

The reference group used in the present study included patients who underwent routine clinical examinations and not healthy volunteers. However, conducting studies on healthy

TABLE 3
Comparison of Percentage Error Between Hypoperfusion Region in Each Disease Group and Same Region in Reference Group for ChangAC Applying μ_{opt}-Value of 0.140 and ChangACSC Applying μ_{opt}-Value of 0.160

			ChangAC			ChangACSC		
Disease	Brain region	Side	Disease	Reference	*P*	Disease	Reference	*P*
AD	Posterior cingulate gyrus	R	0.55 ± 3.49	−0.71 ± 3.04	0.34	−3.71 ± 2.78	−1.76 ± 5.72	0.14
		L	0.52 ± 3.44	0.17 ± 2.48	0.83	−4.85 ± 4.19	−1.97 ± 5.75	0.13
	Medial temporal lobe	R	3.00 ± 3.32	5.82 ± 4.76	0.08	−0.55 ± 4.36	1.89 ± 6.26	0.23
		L	4.83 ± 3.38	6.95 ± 5.03	0.18	2.38 ± 3.64	3.51 ± 6.57	0.83
DLB	Occipital lobe	R	−4.24 ± 3.38	−4.33 ± 2.57	0.89	−7.82 ± 5.09	−7.47 ± 4.97	0.69
		L	−3.33 ± 2.96	−2.89 ± 3.10	0.64	−7.03 ± 4.64	−6.33 ± 3.66	0.44
FTLD	Frontal lobe	R	−3.29 ± 4.34	−3.79 ± 1.41	0.85	−5.15 ± 6.02	−5.26 ± 0.86	0.80
		L	−0.09 ± 4.45	−1.39 ± 2.05	0.56	−1.76 ± 6.75	−2.89 ± 4.25	0.84
	Temporal lobe	R	−2.70 ± 3.48	−3.43 ± 3.16	0.59	−5.98 ± 4.51	−1.45 ± 4.66	0.88
		L	1.64 ± 3.30	1.27 ± 3.26	0.70	−1.45 ± 4.66	−1.88 ± 4.89	0.88
MSA-C	Cerebellum	R	−1.11 ± 5.51	−0.13 ± 3.40	0.69	−6.05 ± 9.54	−8.79 ± 4.63	0.45
		L	0.66 ± 5.83	2.32 ± 3.71	0.36	−3.70 ± 9.93	−6.62 ± 4.76	0.72

AD = Alzheimer disease; DLB = dementia with Lewy bodies; FTLD = frontotemporal lobar degeneration; MSA-C = multiple system atrophy of cerebellar type.
Data are mean ± SD.

volunteers is not practical to determine μ_{opt}-values. Licho et al. (*28*) also evaluated patients who underwent routine clinical examinations to validate the effects of various AC methods. In clinical routine, there are few patients in whom brain perfusion is generally preserved. We included patients diagnosed with a mild degree of nonspecific hypoperfusion in the reference group to obtain a larger cohort of patients for inclusion in the present study. Additionally, including more patients enables more generalizable μ_{opt}-values to be determined.

This study had some limitations. First, it was difficult for all patients to achieve an ideal head tilt because of patient-specific limitations in body position during SPECT imaging. These factors may have influenced the variation of μ_{opt}-values depending on the slice position. Second, the specifications for SC of the SPECT/CT system used in this study were limited to the dual-energy window method only. Since ^{123}I also emits photons with energies of as high as 529 keV, it is best to use a multiple-window method, including the triple-energy-window method, to improve the effects of down scatter. Third, we investigated using one type of γ-camera for ^{123}I with constant parameters for image reconstruction and SC. A preliminary validation using several patients confirmed that the μ_{opt}-values for each patient did not change when the number of iterations for image reconstruction and the weighting factor for SC was changed; however, this was not sufficient. The possibility that μ_{opt}-values may change when other radionuclides, γ-cameras, or other SC are used cannot be extrapolated to other clinical applications. These should be investigated in further studies.

CONCLUSION

We evaluated the μ_{opt}-value for the Chang method using clinical data by comparing it with the CT-based method. The μ_{opt}-values of the Chang method were 0.140 for ChangAC and 0.160 for ChangACSC. It was possible to achieve mean AC accuracies of 4.45% for ChangAC and 6.37% for ChangACSC using μ_{opt}-values.

DISCLOSURE

No potential conflict of interest relevant to this article was reported.

ACKNOWLEDGMENT

We thank Editage (www.editage.com) for English language editing.

KEY POINTS

QUESTION: Can we optimize the μ-value of the Chang method using clinical data?

PERTINENT FINDINGS: In this retrospective study, we determined the μ_{opt}-value for the Chang method by comparing this method with the CT-based method, the gold standard for AC. We found that the μ_{opt}-values were 0.140 for the Chang method without SC and 0.160 for the Chang method with SC, although various μ-values have been used in previous studies.

IMPLICATIONS FOR PATIENT CARE: The Chang method can achieve more accurate AC using our determined μ-values.

REFERENCES

1. Zaidi H, Hasegawa B. Determination of the attenuation map in emission tomography. *J Nucl Med.* 2003;44:291–315.

2. Hayashi M, Deguchi J, Utsunomiya K, et al. Comparison of methods of attenuation and scatter correction in brain perfusion SPECT. *J Nucl Med Technol.* 2005;33: 224–229.
3. Inoue Y, Hara T, Ikari T, Takahashi K, Miyatake H, Abe Y. Super-early images of brain perfusion SPECT using ^{123}I-IMP for the assessment of hyperperfusion in stroke patients. *Ann Nucl Med.* 2018;32:695–701.
4. Ito H, Iida H, Kinoshita T, Hatazawa J, Okudera T, Uemura K. Effects of scatter correction on regional distribution of cerebral blood flow using I-123-IMP and SPECT. *Ann Nucl Med.* 1999;13:331–336.
5. Shiga T, Kubo N, Takano A, et al. The effect of scatter correction on ^{123}I-IMP brain perfusion SPET with the triple energy window method in normal subjects using SPM analysis. *Eur J Nucl Med Mol Imaging.* 2002;29:342–345.
6. Yamashita K, Uchiyama Y, Ofuji A, et al. Fully automatic input function determination program for simple noninvasive ^{123}I-IMP microsphere cerebral blood flow quantification method. *Phys Med.* 2016;32:1180–1185.
7. Ishii K, Hanaoka K, Okada M, et al. Impact of CT attenuation correction by SPECT/CT in brain perfusion images. *Ann Nucl Med.* 2012;26:241–247.
8. Iida H, Nakagawara J, Hayashida K, et al. Multicenter evaluation of a standardized protocol for rest and acetazolamide cerebral blood flow assessment using a quantitative SPECT reconstruction program and split-dose ^{123}I-iodoamphetamine. *J Nucl Med.* 2010;51:1624–1631.
9. Iida H, Narita Y, Kado H, et al. Effects of scatter and attenuation correction on quantitative assessment of regional cerebral blood flow with SPECT. *J Nucl Med.* 1998;39:181–189.
10. Kim KM, Watabe H, Hayashi T, et al. Quantitative mapping of basal and vasareactive cerebral blood flow using split-dose ^{123}I-iodoamphetamine and single photon emission computed tomography. *Neuroimage.* 2006;33:1126–1135.
11. Nicholson R, Doherty M, Wilkins K, Prato F. Paradoxical effects of the skull on attenuation correction requirements for brain SPECT. *J Nucl Med.* 1988;29:1316.
12. Stodilka RZ, Kemp BJ, Prato FS, Nicholson RL. Importance of bone attenuation in brain SPECT quantification [abstract]. *J Nucl Med.* 1998;39:190–197.
13. Van Laere K, Koole M, Versijpt J, Dierckx R. Non-uniform versus uniform attenuation correction in brain perfusion SPET of healthy volunteers. *Eur J Nucl Med.* 2001;28:90–98.
14. Arlig A, Gustafsson A, Jacobsson L, Ljungberg M, Wikkelsö C. Attenuation correction in quantitative SPECT of cerebral blood flow: a Monte Carlo study. *Phys Med Biol.* 2000;45:3847–3859.
15. Law SK. Thickness and resistivity variations over the upper surface of the human skull. *Brain Topogr.* 1993;6:99–109.
16. Kemp BJ, Prato FS, Dean GW, Nicholson RL, Reese L. Correction for attenuation in technetium-99m-HMPAO SPECT brain imaging. *J Nucl Med.* 1992;33:1875–1880.
17. Van Laere K, Koole M, Kauppinen T, Monsieurs M, Bouwens L, Dierck R. Nonuniform transmission in brain SPECT using ^{201}Tl, ^{153}Gd, and ^{99m}Tc static line sources: anthropomorphic dosimetry studies and influence on brain quantification. *J Nucl Med.* 2000;41:2051–2062.
18. Jaszczak RJ, Greer KL, Floyd CE Jr, Harris CC, Coleman RE. Improved SPECT quantification using compensation for scattered photons. *J Nucl Med.* 1984;25: 893–900.
19. Onishi H, Matsutake Y, Kawashima H, Matsutomo N, Amijima H. Comparative study of anatomical normalization errors in SPM and 3D-SSP using digital brain phantom. *Ann Nucl Med.* 2011;25:59–67.
20. Minoshima S, Koeppe RA, Mintun MA, et al. Automated detection of the intercommissural line for stereotactic localization of functional brain images. *J Nucl Med.* 1993;34:322–329.
21. Imran MB, Kawashima R, Sato K, et al. Mean regional cerebral blood flow images of normal subjects using technetium-99m-HMPAO by automated image registration. *J Nucl Med.* 1998;39:203–207.
22. Jonsson C, Pagani M, Johansson L, Thurfjell L, Jacobsson H, Larsson SA. Reproducibility and repeatability of ^{99}Tc^{m}-HMPAO rCBF SPET in normal subjects at rest using brain atlas matching. *Nucl Med Commun.* 2000;21:9–18.
23. Catafau AM, Lomeña FJ, Pavia J, et al. Regional cerebral blood flow pattern in normal young and aged volunteers: a ^{99m}Tc-HMPAO SPET study. *Eur J Nucl Med.* 1996;23:1329–1337.
24. Lillie EM, Urban JE, Lynch SK, Weaver AA, Stitzel JD. Evaluation of skull cortical thickness changes with age and sex from computed tomography scans. *J Bone Miner Res.* 2016;31:299–307.
25. Berger MJ, Hubbell JH. *XCOM: Photon Cross Sections on a Personal Computer.* National Bureau of Standards; 1987. Report NBSIR 87-3597.
26. Zaidi H, Montandon ML. Which attenuation coefficient to use in combined attenuation and scatter corrections for quantitative brain SPET? *Eur J Nucl Med Mol Imaging.* 2002;29:967–969, author reply 969–970.
27. Harris CC, Greer KL, Jaszczak RJ, Floyd CE Jr, Fearnow EC, Coleman RE. Tc-99m attenuation coefficients in water-filled phantoms determined with gamma cameras. *Med Phys.* 1984;11:681–685.
28. Licho R, Glick SJ, Xia W, Pan TS, Penney BC, King MA. Attenuation compensation in ^{99m}Tc SPECT brain imaging: a comparison of the use of attenuation maps derived from transmission versus emission data in normal scans. *J Nucl Med.* 1999;40:456–463.